Anal. Chem. **2006,** *78,* 7206−7210

Mesoscale Energy Deposition Footprint Model for Kiloelectronvolt Cluster Bombardment of Solids

Michael F. Russo, Jr. and Barbara J. Garrison*

104 Chemistry Building, Department of Chemistry, Penn State University, University Park, Pennsylvania 16802

Molecular dynamics simulations have been performed to model 5-keV C_{60} and Au_3 projectile bombardment of an amorphous water substrate. The goal is to obtain detailed insights into the dynamics of motion in order to develop a straightforward and less computationally demanding model of the process of ejection. The molecular dynamics results provide the basis for the mesoscale energy deposition footprint model. This model provides a method for predicting relative yields based on information from less than 1 ps of simulation time.

As computing power continues to grow, so too does the size and sophistication of the systems modeled. This computational growth, however, is still too slow for the multitude of scenarios that one wants to model, and thus, computer power continues to be a bottleneck between the potential knowledge gained from a simulation and the amount of time needed to accomplish it. Due to this fact, it is still advantageous to develop simple models for conceptual and semiquantitative understanding.

One example of this situation is the development and use of cluster over atomic beams in secondary ion mass spectrometry.[1−3] Through the use of molecular dynamics (MD) simulations, considerable insight has been gained into the physical processes that govern these events. For cluster bombardment, the MD computer simulations require on the order of millions of atoms, with one individual cluster impact taking several days to several months of computer time. Thus, testing all the possible conditions of incident energy and angle and all possible different cluster types is virtually impossible with the MD simulations of the full dynamical event for complex systems of experimental interest. The simulations to date do show that there are elements of an almost macroscale-type motion; thus, it is of particular interest to meld both the macro and atomic motions into a model that describes a middle, or mesoscopic, regime.

To understand the physical phenomena that govern the events of kiloelectronvolt cluster bombardment and provide the necessary basis for developing a conceptual and semiquantitative model of the ejection yields, we have performed a comparative molecular dynamics study of two predominant cluster sources, C_{60} and Au_3.[4,5] In this study, we use an amorphous water sample as a model for the low-mass, weakly bound targets typical of organic and biological samples. The mesoscale energy deposition footprint (MEDF) model is developed, which explains the relative yield and ejection volume size and shape differences based on this deposited energy profile. The MEDF model suggests that relative yield information may be achieved through the use of short (<1 ps) simulations.

COMPUTATIONAL DETAILS

Molecular dynamics simulations have been used extensively to study both atomic and cluster bombardment events. The MD scheme utilized here has been explained in detail elsewhere.[6,7] Simulations were performed of C_{60} and Au_3 bombardment using an amorphous water substrate equilibrated to ∼300 K. Both projectiles were given 5 keV of initial kinetic energy and were aimed normal to the surface. The atoms within the incident particles were given initial velocities of zero with respect to their center of mass, and their orientation was determined randomly. One trajectory was performed for both systems, and each was run up to a time of 20 ps. For the C_{60} bombardment, a sample consisting of 1.21 million atoms (400 000 water molecules, ∼3000 Na^+ ions, and ∼3000 Cl^- ions) with dimensions of 29.3 nm × 29.3 nm × 16.1 nm was used. This substrate for Au_3 bombardment measured 16.0 nm × 16.0 nm × 32.5 nm with 242 000 water molecules, ∼2000 Na^+ ions, and ∼2 000 Cl^- ions, for a total of 730 000 atoms. The presence of the Na^+ and Cl^- was due to an initial interest in preformed ions and ultimately turned out to not be a critical part of this analysis. Rigid and stochastic layers were employed for both systems along the sides and bottom to prevent the reflection of pressure waves.[8] The CPU time for each simulation was ∼4 months on a single 2.0-GHz AMD Opteron Processor.

The forces among atoms within the substrate were described by a mix of several different empirical pairwise additive potential functions. The descriptions of these potentials along with their parameters have been described elsewhere.[9,10] The bond lengths

* To whom correspondence should be addressed. E-mail: bjg@psu.edu.

(1) Castner, D. G. *Nature* **2003**, *422*, 129−130.
(2) Winograd, N. *Anal. Chem.* **2005**, *77*, 142A−149A.
(3) Proceedings of the Fifteenth International Conference on Secondary Ion Mass Spectrometry and Related Topics, *Appl. Surf. Sci.* **2006**, *252*, 6403−7326.
(4) Davies, N.; Weibel, D. E.; Blenkinsopp, P.; Lockyer, N.; Hill, R.; Vickerman, J. C. *Appl. Surf. Sci.* **2003**, *203*, 223−227.
(5) Wong, S. C. C.; Hill, R.; Blenkinsopp, P.; Lockyer, N. P.; Weibel, D. E.; Vickerman, J. C. *Appl. Surf. Sci.* **2003**, *203*, 219−222.
(6) Garrison, B. J. *Chem. Soc. Rev.* **1992**, *21*, 155−162.
(7) Garrison, B. J. In *ToF−SIMS: Surface Analysis by Mass Spectrometry*; Vickerman, J. C., Briggs, D., Eds.; Surface Spectra: Manchester, 2001; pp 223−257.
(8) Postawa, Z.; Czerwinski, B.; Szewczyk, M.; Smiley, E. J.; Winograd, N.; Garrison, B. J. *Anal. Chem.* **2003**, *75*, 4402−4407.
(9) Wojciechowski, I.; Sun, J. M.; Szakal, C.; Winograd, N.; Garrison, B. J. *J. Phys. Chem. A* **2004**, *108*, 2993−2998.

10.1021/ac061180j CCC: $33.50
Published on Web 09/21/2006

and angles of the water molecules were held rigid through the use of the RATTLE algorithm.[11] For the atoms in the incident clusters, all interactions with substrate constituents were modeled using a Moliére potential. For Au−Au, we employed a molecular dynamics/Monte Carlo corrected effective medium potential,[12] and for C−C interactions, the REBO potential for hydrocarbons developed by Brenner was used.[13,14]

A large rim is formed around the crater following bombardment; thus, several steps are needed in order to evaluate the ejection yield. A boundary is set above the surface that distinguishes between sputtered material and that is still part of the system. After a sufficient amount of time, the number of particles crossing this boundary to become ejected approaches zero. The boundary is then adjusted to be above the protruding "rim" region of the crater that is formed. This eliminates inclusion of material in the ejecta, which is a significant distance above the original surface, but is still connected to the bulk sample.

RESULTS AND DISCUSSION

Meso- and Microscale Behavior. Cross sections of the two systems at 1 and 20 ps are illustrated in Figure 1. Each time snapshot represents a 2-nm-thick slice down the middle of the full sample, centered on the point of impact. Any atoms outside the slice, including projectile atoms, are not shown. By the end of the first picosecond, nearly all of the kinetic energy of each cluster has been transferred to the substrate, and the impact portion of the event has ended. The large-scale aftereffects of the collision, crater and plume formation, are represented at 20 ps. Both systems are significantly altered by the cluster impact with the formation of a large crater. Although the final craters appear similar, the events giving rise to these mesoscale deformations, however, are different. Therefore, investigation into the atomic-scale behavior of each cluster is needed.

The motion of the projectile atoms is displayed in the time lapse color portion of Figure 1 at 1 ps. Each projectile is represented by 25 snapshots taken at 40-fs intervals from 0 to 1 ps. After only 3−4 frames (80−120 fs), it is evident that both projectiles have begun to break apart. The C_{60} shatters, and the direction of motion of the individual carbon atoms quickly randomizes due to multiple collisions, while the Au_3 slowly drifts apart laterally with all three gold atoms remaining coordinated in their downward momentum. This difference in behavior is primarily due to two main factors: energy per projectile particle and projectile atom mass versus substrate molecular mass. Each carbon atom, having 83.34 eV of kinetic energy and a mass of 12 amu, is traveling with a momentum ~18 times smaller than that of a gold atom, which has a kinetic energy of 1667 eV and a mass of 197 amu. Thus, the carbon atoms are more easily deflected by the 18 amu water molecules and are able to transfer their energy more rapidly.[15] By the end of the first picosecond, all of the

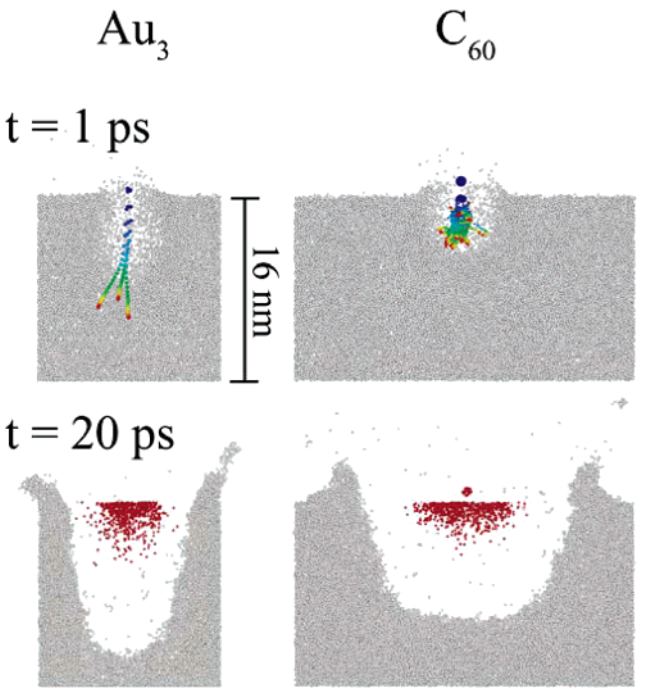

Figure 1. Time snapshots of the Au_3 and C_{60} collision events at 1 and 20 ps. Each image is a 2-nm slice through the center of the substrate. Gray dots represent the Na, Cl, and water molecules, with the hydrogens removed for clarity. The frame at 1 ps contains a time lapse overlay of projectile atomic motion leading up to 1 ps. The colors progress through the rainbow from blue to red with each of the 25 frames separated by 40 fs. The frames at 20 ps display the ejected particles at their original positions in red overlaid on the substrate at 20 ps.

downward momentum of the fullerene molecule has been appreciably reduced and each carbon atom is confined to the evacuated crater region of 4 nm deep or less. Conversely, the gold atoms are 11 times heavier than the water and cannot be significantly deflected by the substrate molecules. They therefore maintain their high velocity and travel a greater distance into the sample. All three gold atoms embed in the bulk of the sample, coming to rest at ~10 nm deep.

Even though the motion of the projectiles is different, the configuration of the systems at 20 ps shows a similarity in the volumes of removed material and the overall evacuated regions. Although a large crater has been formed for both systems, the ejected atoms, shown in red at their original positions in the system, are much closer to the surface. This difference is due to the large downward component of momentum of the original projectile, which is being transferred to the weakly bound system. The substrate recoils from the impact and generates a buildup of density around the crater, which propagates downward expanding the crater until the internal pressure is sufficient to stop its advancement. The ability to create this density "wall" may be the defining characteristic that restricts C_{60} to the near-surface crater region. We hypothesize that the substrate will return to a near-initial state and close up much of the crater; however, after running the C_{60} simulation additionally to 45 ps, we saw no appreciable "healing" and believe that this action occurs on a much longer time scale than is feasible to simulate at this time.

The bifurcation of the motion of the system into the molecules moving upward toward the vacuum and the downward motion

(10) Wojciechowski, I. A.; Kutliev, U.; Sun, S. X.; Szakal, C.; Winograd, N.; Garrison, B. J. *Appl. Surf. Sci.* **2004**, *231−2*, 72−77.
(11) Andersen, H. C. *J. Comput. Phys.* **1983**, *52*, 24−34.
(12) Kelchner, C. L.; Halstead, D. M.; Perkins, L. S.; Wallace, N. M.; Depristo, A. E. *Surf. Sci.* **1994**, *310*, 425−435.
(13) Brenner, D. W. *Phys. Rev. B* **1990**, *42*, 9458−9471.
(14) Brenner, D. W.; Shenderova, O. A.; Harrison, J. A.; Stuart, S. J.; Ni, B.; Sinnott, S. B. *J. Phys.: Condens. Matter* **2002**, *14*, 783−802.
(15) Szakal, C.; Kozole, J.; Russo, M. F.; Garrison, B. J.; Winograd, N. *Phys. Rev. Lett.* **2006**, *96*, 216104.

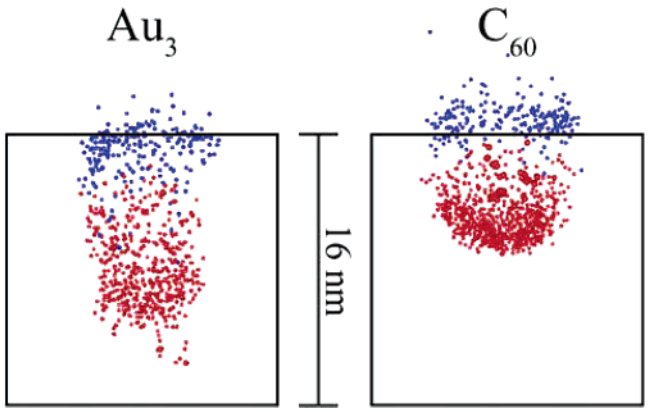

Figure 2. Vertical motion of water molecules at 1 ps. Red and blue dots represent atoms, which have moved more than 0.5 nm toward the bulk and vacuum, respectively.

forming the crater begins in the very early stages of the mesoscale motion.[16] The upward and downward motion at 1 ps is shown in Figure 2, where red dots indicate molecules that are moving into the bulk and blue dots represent molecules moving toward the vacuum. Any molecules that have moved more than 0.5 nm in the vertical direction within the first picosecond are shown. This figure, together with the 20-ps frames of Figure 1, shows evidence of a boundary approximately 2−3 nm deep at which a bifurcation of upward and downward motion occurs following the cluster bombardment. Additionally, from the shape of the ejected volumes seen in Figure 1, at 20 ps there appears to be a radial point of origin centered at the intersection of this bifurcation line and the axis of cluster impact. All ejected material for both systems must therefore originate in the near-surface region of the sample roughly 2−3 nm deep or less in order to obtain upward velocity, and within a conical volume that acquired sufficient energy to be liberated and thus sputtered. This suggests that the transfer of energy within this 3-nm-thick zone is an important aspect of a cluster's behavior toward generating sputtered material and necessitates a closer look at this region.

MEDF Model. The conical ejection volume is reminiscent of the ejection volume from an energized cylindrical track as described in fluid dynamics calculations of megaelectronvolt (MeV) particle bombardment performed by Jakas et al.[17] In their model, the energized track is initiated as an excitation of the bulk material along the path of the projectile as shown in Figure 3a. The excitation track has a characteristic radius (R_{cyl}) centered along the impact axis and an average excitation energy, $\tilde{E} = (E_{exc}/U_o)$ above the cohesive energy, U_o, of the substrate.[17] As Jakas et al. explained, there is a quick but powerful displacement of the side and upper boundaries of this track that energizes the particles within the volume. Only those particles that are near the surface at a depth of R_{cyl} or less will be able to "feel" this displacement of the upper limit and be able to expand toward the vacuum and escape.[17] All other particles R_{cyl} deep and below will be surrounded by bulk particles and only be able to expand horizontally and downward into the bulk. As time moves forward and the material starts to eject, this idea breaks down, and the opening created by

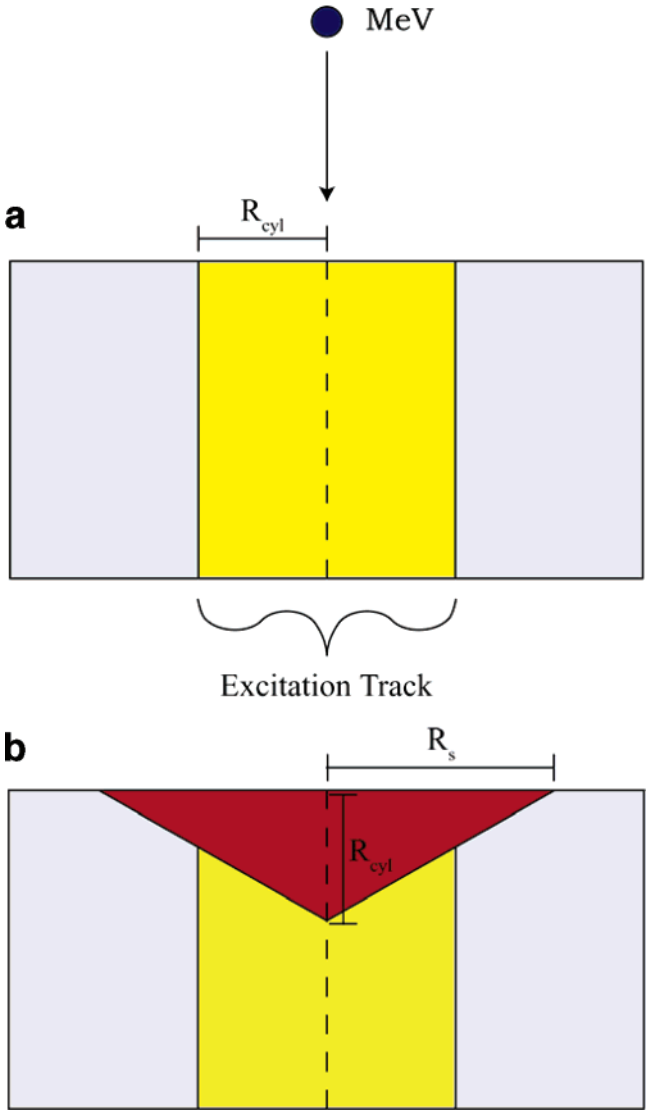

Figure 3. Diagram of the ejection model developed by Jakas et al.[17] (a) The yellow region represents the excitation track. (b) The red area is the ejection cone as described in the text.

the evacuated material increases the contact with the vacuum and allows for further ejection from areas farther out within a radius of R_s, where $R_s = (\tilde{E})^{1/2}R_{cyl}$.[17] This leads to a simple prediction of the total yield, $Y = n_o(\pi/3)R_s^2R_{cyl}$ or $Y = n_o(\pi/3)R_{cyl}^3\tilde{E}$, which is equal to the volume of the red cone in Figure 3b multiplied by the number density, n_o.[17] From this equation, only the size and average excitation relative to the substrate's intermolecular binding energy in this collision zone (hereinafter called footprint) are needed to estimate a yield for a particular system.

The MeV process is one in which the incident ion creates an electronic excitation along a long track and energizes a cylindrical region as shown conceptually in Figure 3. The main issue is whether the cluster bombardment event creates something akin to an energized track because the cluster deposits its energy over a time period rather than near instantaneously. For the analysis here, we have plotted the energy each projectile transfers to the substrate versus time and chose a time when the incident particle had deposited 90% of its energy, 4500 eV, into the substrate (see Figure 4). For C_{60} bombardment, this time is 130 fs, and for the

(16) Wojciechowski, I. A.; Garrison, B. J. *J. Phys. Chem. A* **2006**, *110*, 1389−1392.
(17) Jakas, M. M.; Bringa, E. M.; Johnson, R. E. *Phys. Rev. B* **2002**, *65*, 165425.

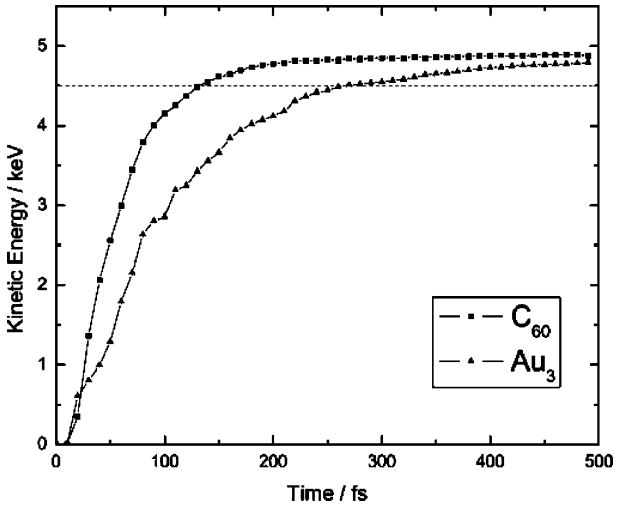

Figure 4. Energy deposition of the projectile into the substrate as a function of time. The horizontal dashed line is at 4500 eV or 90% of the initial projectile energy.

Au_3 bombardment, it is 260 fs. The excitation energy at these times in a slice of the sample centered about the impact area is shown in Figure 5 for both projectiles. For this representation, the kinetic energy associated with upward and downward motion of the water molecules has been removed so that the energy is more comparable to the fluid dynamics calculation. As is observed in Figure 3, the energy deposition does appear to be "tracklike" in the near-surface region and is an indication that the initiation of the crater formation is a mesoscale event rather than a collision cascade.[18] The value of R_{cyl}, however, is hard to define but in both cases is ~2 nm. As a guide to the eye, lines have been drawn in Figure 5 to designate a radius of ~2 nm and a depth of ~2 nm from the surface.

The difference in depth at which the two projectiles deposit their energy is clear from Figure 5. A considerable amount of the energy deposited by the C_{60} is within a depth predicted by the fluid dynamics model to be productive for ejecting material. On the other hand, the Au_3 deposits its energy too deep and over too large an area for it to contribute effectively to ejection. Thus, a sizable fraction of the incident Au_3 energy is wasted in terms of promoting ejection of material. Even though the energy deposition is not uniform across the energized near-surface ejection region, it is possible to make an estimate of the amount of energy deposited. For Au_3, the relative excitation energy is slightly greater than 1; thus, the radius of the cone of material ejected should be a bit larger than R_{cyl}. On the other hand, for C_{60}, the relative excitation energy is ~3; thus, the radius of the cone of material ejected is $\sim(3)^{1/2}R_{cyl}$. Cones with these dimensions have been inscribed in Figure 5 to show the comparison with the actual initial positions of the ejected atoms.

The essence of the physics of the cluster bombardment and the essence of the mesoscale energy deposition footprint model is that there is a fast mesocale energy deposition in a footprint region of the sample. The energized region undergoes a fluidlike motion giving rise to the ejection of material. By examining the energy deposition region with MD simulations, the values of R_{cyl} and $\tilde{E}$ can be estimated. The total yield is given by $Y = n_o(\pi/3)$-

(18) Garrison, B. J. *Appl. Surf. Sci.* **2006**, *252*, 6409−6412.

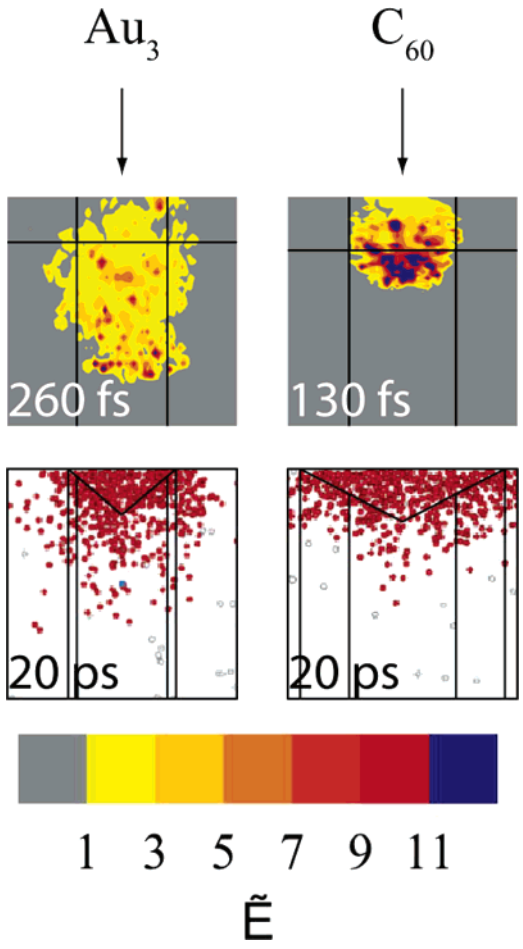

Figure 5. Analysis of excitation track and ejection cone. The top figures give the excitation energy in a 2-nm slice of the system at the time when 90% of the energy has been deposited. The lines represent the estimate of R_{cyl} of 2 nm. The bottom figures show the original position of the ejected atoms in red, that is, the same information as in the 20-ps snapshot of Figure 1. The lines illustrate R_{cyl}, R_s, and the difference in the ejection cone shape for each projectile as discussed in the text.

Table 1. Calculated Yields at 20 ps

projectile	Au	C	H_2O	Na^+	Cl^-
Au_3	0		998	10	3
C_{60}		16	1644	12	6

$R_{cyl}{}^3\tilde{E}$, the depth of origin of the material is R_{cyl}, and the radial extent of the ejected material at the surface is $R_s = (\tilde{E})^{1/2}R_{cyl}$.

The MEDF model predicts that C_{60} will have a much broader, flatter ejection area when compared to that of Au_3, and the results of Figure 5 support this prediction. The model also predicts that C_{60} should eject more particles than Au_3, a condition that is also predicted by the MD simulations as given in Table 1. For completeness in Table 1, the Na^+ and Cl^- yields are given even though their yields are not part of this discussion.[9,10] A quantitative comparison between the MD yields and the MEDF model is tricky, however. The predicted yield depends on the cube of R_{cyl}. Any imprecision in this value makes a relatively large difference in the predicted yield. In addition, the deposited energy is not uniform and estimating its value cannot be done exactly. There are, of course, deviations as the MD simulations follow all collision

molecular motions and not just those associated with fluid flow. In particular, for the Au_3 case, there are many atoms that eject from the energized region below the cone, as seen in Figure 5.

The comparison of the fluid dynamics model to the MD simulations introduces a dimension, R_{cyl}, over which the energy of the cluster beam is deposited. This footprint of energy deposition is much larger than either cluster size. For example, the diameter of C_{60} is only 0.7 nm whereas the footprint diameter is 4 nm. The gold cluster, although smaller than the fullerene molecule, appears to also have a footprint of 4 nm. This footprint size reflects the distance that energy can flow in the material in the short time that the cluster deposits its energy and is not the size of the actual projectile cluster.

The utility of the MEDF model to the understanding of cluster bombardment is in the ability to use information from short-time MD simulations as in Figure 5 to predict relative yields of material ejection. Although simulations have been performed for argon clusters bombarding solid argon for a variety of initial energies,[19,20] performing comparable calculations for potentials representing substrates of experimental interest such as amorphous water or solid benzene[21] are prohibitive. In fact, the choice of an initial kinetic energy for the simulations presented here was restricted to 5 keV in order to maintain a computationally feasible sample size. From examining short-time energy deposition profiles for C_{60} and Au_3 bombardment on amorphous water as a function of various incident energies, it is possible to predict the experimental yield trends using a smaller substrate than would be needed for a full simulation.[22] Similarly, the MEDF model has been used to explain yield trends of a variety of fullerene clusters bombarding a benzene solid.[23]

CONCLUSIONS

The results presented above shed light on phenomena associated with cluster bombardment. Although both C_{60} and Au_3 have remarkably similar mesoscopic impacts on the substrate, several microscopic mechanisms separate these two projectiles. Both the number of constituent atoms, which affects mass and thus momentum per particle, and the mass difference (mass match) between the projectile and substrate play a key role in the events of an impact. The fullerene C_{60} splits apart sending carbon atoms in all directions, which quickly transfer energy in a spherical manner, maximizing excitation in the near-surface region of ejection. The metal cluster Au_3 cannot be deflected by the much lighter substrate molecules and embeds into the sample, distributing its energy more slowly in a long path. This deep penetration causes energy to be wasted by transferring it into areas too far from the surface to facilitate ejection.

The MEDF model for the ejection of substrate material has been proposed based on fluid dynamics calculations. Using the MEDF model of ejection as a guide, it is possible to determine relative yields for these systems, as well as relative efficiency of each projectile. While this method is qualitative in nature at this point, there is still a great deal of information that can be deduced with little initial details. Nearly all projectile energy is transferred to the substrate within the first quarter picosecond. This allows the necessary information to be obtained in a short amount of time and eliminates the need for large samples and long simulations since only a small volume is affected in the early stages of bombardment. In the future, better methods for determining footprint size and excitation energy should lead to a more quantitative analysis, which can be used to predicts yields as a function of experimental conditions (e.g., incident energy, angle, and projectile type) in a matter of hours or days, rather than weeks or months of simulation time.

(19) Anders, C.; Urbassek, H. M. *Phys. Rev. B* **2004**, *70*, 155404.
(20) Anders, C.; Urbassek, H. M. *Nucl. Instrum. Methods Phys. Res., Sect. B* **2005**, *228*, 84−91.
(21) Smiley, E. J.; Postawa, Z.; Wojciechowski, I. A.; Winograd, N.; Garrison, B. J. *Appl. Surf. Sci.* **2006**, *252*, 6436−6439.
(22) Russo Jr., M. R.; Szakal, C.; Kozole, J.; Winograd, N.; Garrison, B. J. Unpublished 2006.
(23) Smiley, E. J.; Winograd, N.; Garrison, B. J. Submitted to *Anal. Chem.*

ACKNOWLEDGMENT

The authors thank the Chemistry Division of the National Science Foundation for their support of this research. We also acknowledge Professor Zbigniew Postawa for his insight and helpful discussion.

Received for review June 29, 2006. Accepted August 17, 2006.

AC061180J